Switching by Photochemical trans–cis Isomerization of Azobenzene Substituents in Organoplatinum Complexes

DATASET *in* ORGANOMETALLICS · AUGUST 2012

Impact Factor: 4.13 · DOI: 10.1021/om3005405

3 AUTHORS, INCLUDING:

Mohamed E. Moustafa
The University of Western Ontario
10 PUBLICATIONS **32** CITATIONS
SEE PROFILE

Richard J Puddephatt
The University of Western Ontario
702 PUBLICATIONS **17,787** CITATIONS
SEE PROFILE

ORGANOMETALLICS

Article

pubs.acs.org/Organometallics

Switching by Photochemical *trans*−*cis* Isomerization of Azobenzene Substituents in Organoplatinum Complexes

Mohamed E. Moustafa, Matthew S. McCready, and Richard J. Puddephatt*

Department of Chemistry, University of Western Ontario, London, Canada N6A 5B7

Supporting Information

ABSTRACT: A diimine ligand, LL = 2-$C_5H_4NCH{=}N$-4-$C_6H_4N{=}NPh$, which carries a *trans*-azobenzene substituent, forms the dimethylplatinum(II) complex $[PtMe_2(LL)]$, which undergoes *trans* oxidative addition with MeI, $PhCH_2Br$, Br_2, and I_2 to give the corresponding organoplatinum(IV) complexes $[PtIMe_3(LL)]$, $[PtBrMe_2(CH_2Ph)(LL)]$, $[PtBr_2Me_2(LL)]$, and $[PtI_2Me_2(LL)]$, respectively. The ligand and the platinum(II) and platinum(IV) complexes are shown to undergo *trans*−*cis* isomerization of the azobenzene substituent upon irradiation, and the *cis* isomers then underwent slow thermal isomerization back to the more stable *trans* isomers.

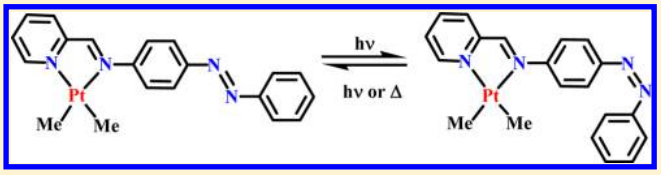

INTRODUCTION

The design and synthesis of organic materials that possess photoswitching ability has been the focus of considerable interest, because these molecular materials have potential applications in areas ranging from pharmaceuticals to optical data storage and photoswitching devices.[1−3] There are many photochromic molecules, including derivatives of spiropyrans, fulgides, diarylethenes, and stilbenes,[4−7] but azobenzenes have attracted particular interest because of their ease of synthesis, their high stability, and their UV−visible absorbance over a wide range of wavelengths.[8] Azobenzene normally exists as the *trans* isomer, which undergoes *trans*−*cis* isomerization upon irradiation with UV light, while the back process can be achieved either by heat or by irradiation with visible light. The *trans*−*cis* photoisomerization process is accompanied by a structural change in which the distance between *para* carbon atoms in azobenzene decreases from 9 to 5.5 Å (Scheme 1), and it is this structural change that can lead to a change in chemical or physical properties and forms the basis of the photoswitching ability.[8]

The synthesis of transition-metal complexes with azo substituents has attracted interest in order to combine the remarkable photoswitching property of azobenzene with the magnetic, electrochemical, catalytic, or biological properties of the metal complex.[9] In many of the known complexes, the azo ligand is chelated to the metal through one of the nitrogen atoms and either a second nitrogen donor substituent or a carbon atom, so that photoisomerization of the azobenzene group is not possible.[9−11] Few transition-metal complexes,[12] and even fewer organometallic complexes,[13] are known in which the azo group is free to undergo photoisomerization. Some of these are illustrated in Chart 1, illustrating that the azo group can be incorporated either into the organometallic unit itself or into a supporting ligand.

Scheme 1. Photoisomerization of Azobenzene

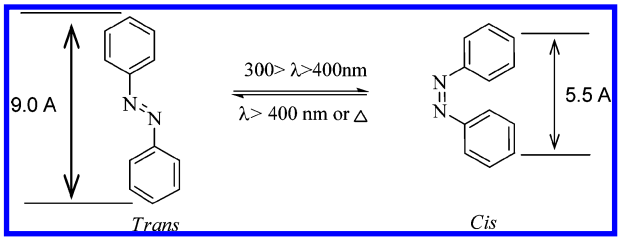

Chart 1. Some Photoswitchable Organometallic Compounds

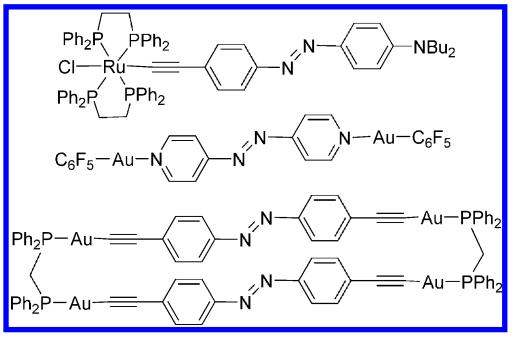

The introduction of functional groups into organoplatinum compounds has been an enduring interest,[14] and we wished to explore the range of methods that could be used to introduce azo groups into organoplatinum complexes and to discover how the organometallic group might influence the *trans*−*cis* isomerization of the azo group. In this context, the synthesis and properties of complexes of both platinum(II) and platinum(IV), which contain a diimine ligand with an azo group substituent, are reported.

Received: June 17, 2012
Published: August 16, 2012

dx.doi.org/10.1021/om3005405 | *Organometallics* 2012, 31, 6262−6269

RESULTS AND DISCUSSION

Synthesis and Characterization of [PtMe$_2$(LL)]. The diimine ligand LL = 2-C_5H_4NCH═N-4-C_6H_4N═NPh, which carries a *trans*-azobenzene substituent, was prepared as an orange solid by the reaction of 4-aminoazobenzene with pyridine-2-carboxaldehyde.[15] The complex [$PtMe_2$(LL)] (**1**) was then prepared by reaction of the ligand LL with [$Pt_2Me_4(\mu$-$SMe_2)_2$],[16] with displacement of the dimethyl sulfide ligands (Scheme 2). Complex **1** was isolated as a violet solid. In the ^{1}H NMR spectrum, it gave two methylplatinum resonances at δ 0.93 and 1.31, each with coupling constant $^2J_{PtH}$ = 88 Hz. In addition, the *ortho* hydrogen atom of the pyridine ring gave a doublet resonance at δ 9.53, with coupling $^3J_{PtH}$ = 22 Hz, and the imine (CH═N) group gave a singlet resonance at δ 9.85, with coupling constant $^3J_{PtH}$ = 30 Hz, demonstrating chelation of platinum(II) by the diimine group (Figure 1).

Scheme 2. Synthesis of Dimethylplatinum(II) Complex 1

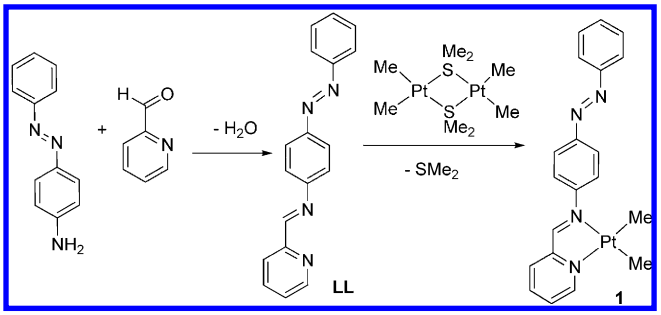

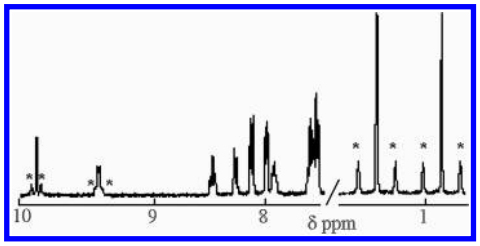

Figure 1. ^{1}H NMR spectrum (400 MHz, acetone-d_6) of complex **1**. ^{195}Pt satellite spectra are indicated by asterisks.

Oxidative Addition Reactions To Give Platinum(IV) Derivatives. Several organoplatinum(IV) complexes were prepared by oxidative addition of halogens or alkyl halides to complex **1**, as shown in Scheme 3.

Scheme 3. Oxidative Addition Reactions of Complex 1

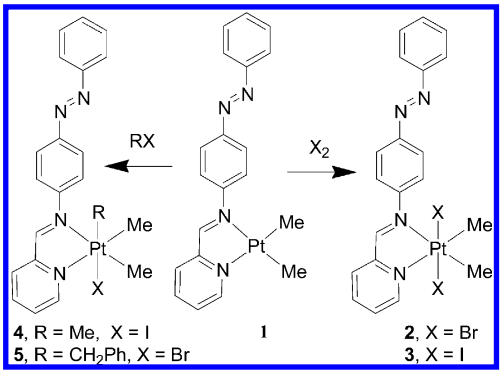

The bromine adduct **2** and iodine adduct **3** were each isolated as brown solids. Only the *trans* adducts were observed (Scheme 3). We note that either *trans* or mixtures of *trans* and *cis* adducts have been observed with other diimine ligands, though the kinetically controlled product is the *trans* isomer.[17] For example, complex **2** gave only two equal-intensity methylplatinum resonances at δ 1.77 and 2.06, each with coupling constant $^2J_{PtH}$ = 73 Hz. The structures were confirmed crystallographically, and the structure of complex **2** is shown in Figure 2. The structure confirms the octahedral stereochemistry at platinum(IV), with mutually *trans* bromine atoms, and the expected *trans* stereochemistry of the azo group.

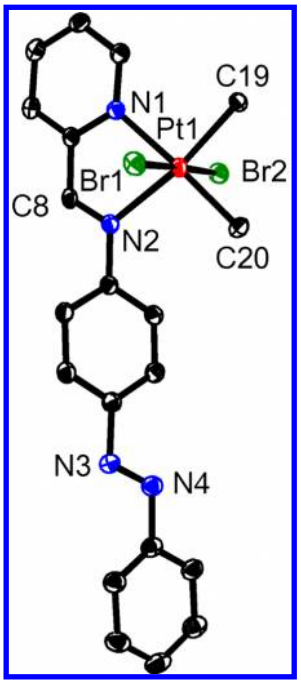

Figure 2. View of the structure of the complex **2**. Selected bond lengths (Å): Pt(1)–N(1), 2.169(3); Pt(1)–N(2), 2.203(4); Pt(1)–Br(1), 2.4430(5); Pt(1)–Br(2), 2.4500(5); Pt(1)–C(19), 2.080(4); Pt(1)–C(20), 2.070(3); N(3)–N(4), 1.253(5).

The structure of complex **3** is similar, as illustrated in Figure 3. However, the complex crystallized with a molecule of iodine bridging between two molecules of complex **3**, giving a Pt–I···I–I···IPt unit, in which the distance I(3A)–I(3B) = 2.747(1) Å is longer than in free iodine (2.667(2) and 2.715(6) Å in the gas and solid, respectively)[18] and the secondary bonding distance I(2)···I(3A) = 3.449(1) Å. This secondary bonding interaction is probably responsible for the bond distance Pt(1)–I(2) = 2.658(6) Å being longer than Pt(1)–I(1) = 2.626(6) Å. The different packing also leads to greater twisting of the aryl groups out of the plane of the azo group in **3** in comparison to **2** (torsion angles N(3)N(4)C(13)C(18) = 10.8(6) and 16.6(9)° and N(4)N(3)C(10)C(11) = 1.6(6) and 12.8(6)° in **2** and **3**, respectively).

The alkyl halide adducts [$PtIMe_3$(LL)] (**4**) and [$PtBrMe_2(CH_2Ph)$(LL)] (**5**) (Scheme 3) were isolated as pale brown solids. The ^{1}H NMR spectrum of **4** contained three methylplatinum resonances at δ 0.65, $^2J_{PtH}$ = 72 Hz, assigned to the axial methyl group, and at δ 1.18 and 1.52, with coupling constants of 72 and 73 Hz, respectively, assigned to the equatorial methyl groups. The imine resonance was at δ 9.48,

dx.doi.org/10.1021/om3005405 | *Organometallics* 2012, 31, 6262–6269

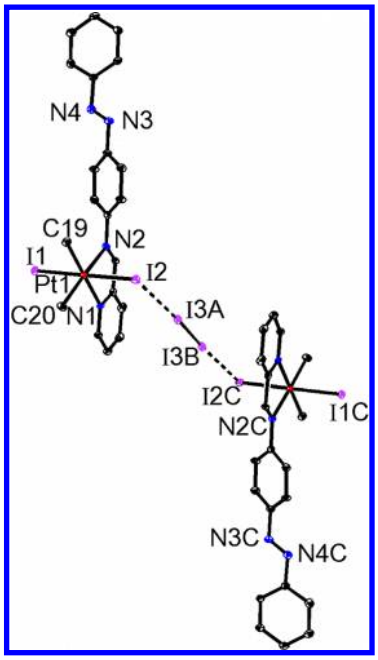

Figure 3. View of the structure of complex **3**. Selected bond lengths (Å): Pt(1)−N(1), 2.170(6); Pt(1)−N(2), 2.193(5); Pt(1)−I(1), 2.626(6); Pt(1)−I(2), 2.658(6); Pt(1)−C(19), 2.064(9); Pt(1)−C(20), 2.073(6); N(3)−N(4), 1.256(8).

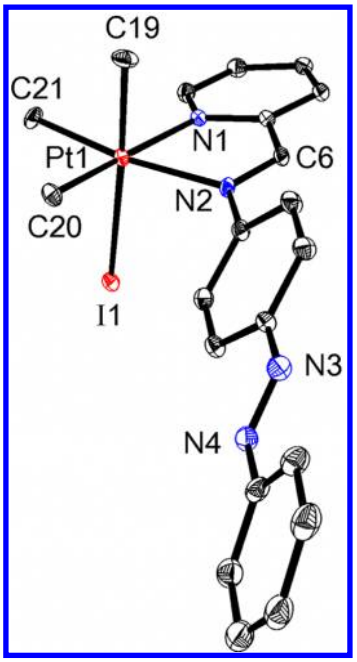

Figure 4. View of the structure of [PtIMe$_3$(LL)] (**4**). Selected bond lengths (Å): Pt(1)−N(1), 2.184(6); Pt(1)−N(2), 2.206(5); Pt(1)−I(1), 2.806(9); Pt(1)−C(19), 2.076(8); Pt(1)−C(20), 2.079(8); Pt(1)−C(21), 2.088(7); N═N, 1.264(8).

$^3J_{PtH}$ = 27 Hz, while the pyridyl proton H^6 was at δ 9.06, $^3J_{PtH}$ = 18 Hz. The ^{1}H NMR spectrum of **5** contained two methylplatinum resonances at δ 1.23 and 1.52, with coupling constants $^2J_{PtH}$ = 72 and 73 Hz, as expected for equatorial methyl groups, while the protons of the CH_2 unit of the benzyl group are diastereotopic and appeared as an AB quartet at δ 2.65, $^2J_{HH}$ = 14 Hz, $^2J_{PtH}$ = 78 Hz and δ 2.80, $^2J_{HH}$ = 14 Hz, $^2J_{PtH}$ = 96 Hz.

The structure of complex **4** is shown in Figure 4. It shows the expected octahedral stereochemistry at platinum(IV) and a roughly planar *trans*-azobenzene group. Notably, the distance Pt(1)−I(1) = 2.806(9) Å in **4** is significantly longer than the distances Pt(1)−I(1) = 2.626(6) Å and Pt(1)−I(2) = 2.658(6) Å in complex **3**, due to the high *trans* influence of the methyl group in **3**. There are two short intermolecular CH···I contacts, which probably represent weak hydrogen bonds to this I(1) atom and which will play a role in the crystal packing.

A comparison of the conformations of different derivatives is given in Table 1, and values calculated by using DFT are given for comparison. The functional BLYP was used because it gives a good treatment of the heavy atom platinum, but it is a compromise, since it may not give the best agreement for bonds between lighter atoms. The experimental data for complexes **2**–**4**, and the DFT calculations for all complexes, indicate significant twisting of the azobenzene substituent out of the diimine plane (Φ1 in Table 1) in order to minimize steric interactions. This twisting will reduce conjugation between the unsaturated diimine and azobenzene groups. The theory predicts that the *trans*-azobenzene unit itself should be very close to planar (Table 1, Φ2 and Φ4 close to zero, Φ3 close to 180°);[8] therefore, the somewhat larger distortions observed, especially for complex **3**, are attributed to packing effects in the crystals. Much larger distortions are predicted for the *cis*-azobenzene derivatives (Table 1), due to steric effects (Scheme 1),[8] but we have not been able to grow crystals to compare theory and experiment in this case. Conjugation between the unsaturated N═N, C_6H_4, and C_6H_5 groups will therefore be decreased in the *cis*-azobenzene derivatives and the N═N distance was calculated to be shorter by about 0.02 Å in the *cis*-azobenzene isomers as a result of this effect.

Table 1. Experimental and Calculated Conformational Parameters

	Φ1[a]	Φ2[a]	Φ3[a]	Φ4[a]
trans-LL[b]	47	2	178	1
[PtMe$_2$(LL)][b]	58	4	180	3
[PtBr$_2$Me$_2$(LL)][b]	62	3	180	1
[PtBr$_2$Me$_2$(LL)][c]	54	2	179	11
[PtI$_2$Me$_2$(LL)][b]	62	3	180	1
[PtI$_2$Me$_2$(LL)][c]	54	13	177	17
[PtIMe$_3$(LL)][b]	59	4	180	3
[PtIMe$_3$(LL)][c]	44	9	179	7
cis-LL[b]	42	34	11	54
[PtMe$_2$(LL)][b]	50	29	10	57
[PtIMe$_3$(LL)][b]	47	34	11	50
[PtBr$_2$Me$_2$(LL)][b]	50	31	10	60
[PtI$_2$Me$_2$(LL)][b]	46	34	6	55

[a]Torsion angles: Φ1 = C═N−C═C (imine-C_6H_4), Φ2 = C═C−N═N (C_6H_4-azo), Φ3 = C−N═N−C, Φ4 = N═N−C═C (azo-C_6H_5). [b]DFT value. [c]Experimental value.

Photoisomerization Studies. The UV−visible spectra of the *trans* and *cis* isomers of azobenzene contain bands from π−π* transitions at ca. 320 and 270 nm, respectively, and weaker bands from symmetry-forbidden n−π* transitions at ca. 450 nm in each case. Irradiation into either band can give *trans*−*cis* isomerization, and the key to photoswitching is that the π−π* transition is more intense for the *trans* isomer while the n−π* transition is more intense for the *cis* isomer. Hence, irradiation at 365 and 450 nm leads to *trans*−*cis* and *cis*−*trans* isomerization, respectively.[8] The frontier orbitals for the two

dx.doi.org/10.1021/om3005405 | *Organometallics* 2012, 31, 6262−6269

isomers of the ligand LL are shown in Figure 5. The only significant change from free azobenzene is that the π^* LUMO

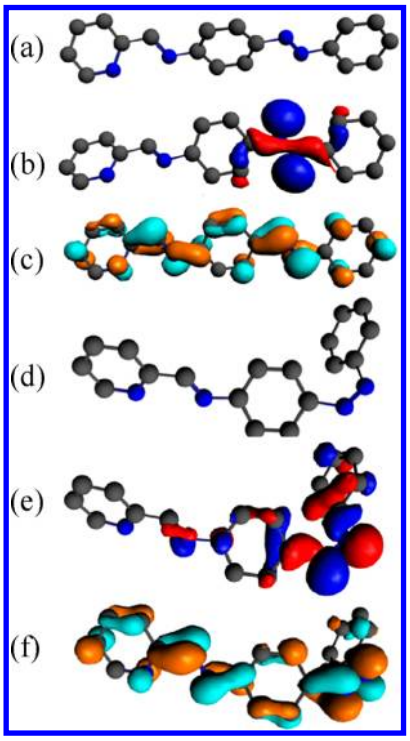

Figure 5. (a) Calculated structure of the ligand *trans*-LL and (b) its HOMO and (c) its LUMO and (d) calculated structure of the ligand *cis*-LL and (e) its HOMO and (f) its LUMO.

is delocalized over both the azobenzene and diimine groups (Figure 5c,f).[8] The *trans* isomer is calculated to be lower in energy than the *cis* isomer by 50 kJ mol^{-1}.

The interest in the present work is on the possible effects of coordination of the diimine ligand to the heavy transition metal in complexes **1**–**5**. Before the photoisomerization reactions were monitored, samples were dissolved in acetonitrile and kept in the dark for 1 day at room temperature to ensure that all azobenzene substituents exist in the more stable *trans* isomeric form. The changes in UV–visible spectra during irradiation of the ligand LL in dichloromethane solution are shown in Figure 6. The π–π^* transition of the *trans* isomer has a maximum absorption at 365 nm, and the n–π^* transition is weak. On irradiation at 365 nm, the π–π^* peak decreased in intensity and the n–π^* band of the *cis* isomer at 490 nm

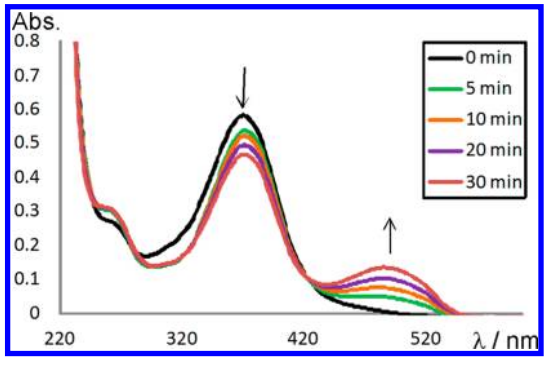

Figure 6. Changes in the UV–visible absorption spectra during irradiation of the ligand LL.

increased in intensity. The isomerization was essentially quantitative, as is typical for azobenzene derivatives.[8]

The changes in UV–visible spectra during irradiation of a solution of complex **1** in acetonitrile, by using UV light at 365 nm, are shown in Figure 7. Complex **1** exhibited a characteristic

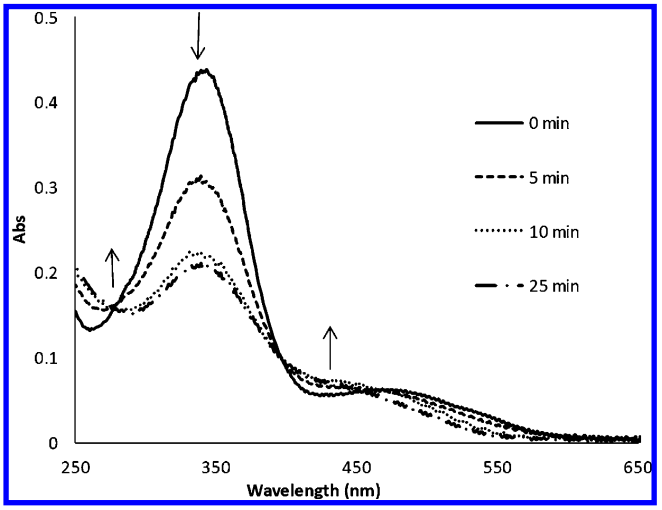

Figure 7. Absorption spectrum of complex [$PtMe_2$(LL)] (**1**) in acetonitrile at 1.56 μM concentrations for *trans*–*cis* photoisomerization upon illumination with UV light at 365 nm.

absorption band centered at 345 nm attributed to the intense π–π^* transition, shifted from 365 nm in the free ligand (Figure 6).[8,15] However, it also gave overlapping broad bands centered at 480 and 530 nm, which probably arise mostly from the Pt(5d)–π^* MLCT transitions rather than the n–π^* transition of the azobenzene group.[19] Upon illumination with 365 nm light, the spectral changes were consistent with the *trans*–*cis* isomerization shown in Scheme 4. There was a decrease in the

Scheme 4. Photoisomerization of [$PtMe_2$(LL)] (1)

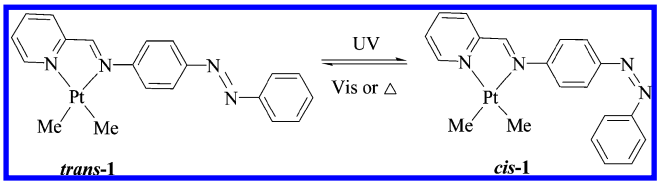

intensity of the π–π^* band of *trans*-**1** at 345 nm accompanied by the appearance of a new band at 430 nm, assigned as mostly due to the n–π^* band of *cis*-**1**. The intensities of the bands assigned to the Pt(5d)–π^* MLCT transitions of *trans*-**1** at 480 and 530 nm decreased markedly during the reaction (Figure 6). The observation of isosbestic points is consistent with a simple isomerization reaction, but the reaction did not proceed to completion (Figure 6), presumably because the back reaction also occurs under the experimental conditions used. If the irradiated sample solution was stored in the dark for 1 day, the original spectrum was recovered, showing that the reverse *cis*–*trans* isomerization can be effected either photochemically or thermally.

Figure 8 shows the calculated structures (Figure 8a,e) and some of the frontier orbitals for the *trans* and *cis* isomers of complex **1**. The isomer *trans*-**1** is calculated to be 50 kJ mol^{-1} more stable than *cis*-**1**, the same value as for the free ligand, indicating that the incorporation of the dimethylplatinum group

dx.doi.org/10.1021/om3005405 | *Organometallics* 2012, 31, 6262–6269

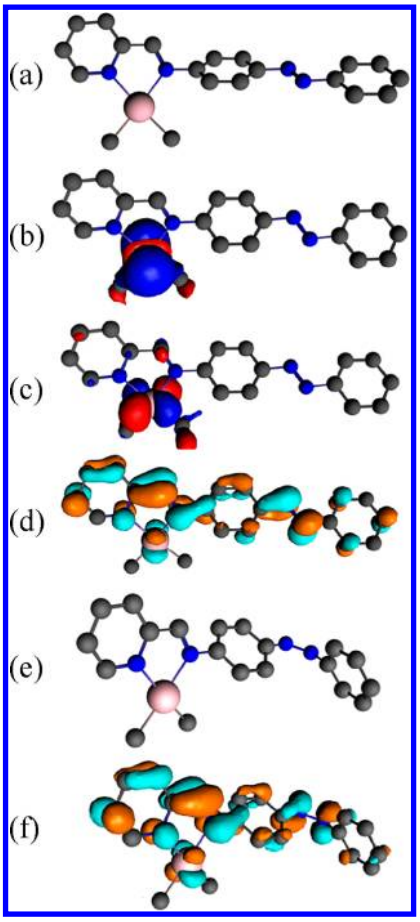

Figure 8. (a) Calculated structure of the complex [$PtMe_2$(LL)] (*trans*-**1**) and (b) its HOMO, (c) its HOMO-1, and (d) its LUMO and (e) calculated structure of the isomer *cis*-**1** and (f) its LUMO.

has very little effect on the thermodynamics of the *trans*−*cis* isomerism. The HOMO for *trans*-**1** has mostly platinum $5d_{z^2}$ character, and the $5d_{\pi}$ orbitals also lie above the highest n(N) orbital level, which is the HOMO in the free ligand (Figure 8b,c). The LUMO is a complex π^* molecular orbital, which is delocalized over both the diimine and azobenzene groups (Figure 8d). These features are similar for the *cis* isomer (Figure 8f).

Figure 9 shows changes in UV−visible spectra during the similar photoisomerization of the platinum(IV) complex **2**.

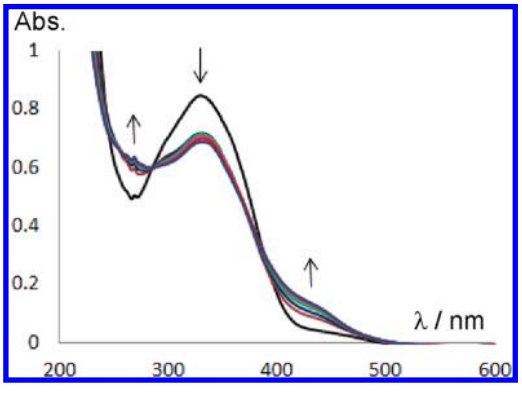

Figure 9. Changes in the absorption spectrum of complex [$PtBr_2Me_2$(LL)] (**2**) in acetonitrile at 1.18 μM concentration during *trans*−*cis* photoisomerization upon irradiation at 365 nm.

Again, the reaction was characterized by a decrease in the intensity of the $\pi-\pi^*$ transition for *trans*-**2**, centered at 339 nm, and an increase in the intensity of the n−π^* transition for *cis*-**2**, centered at 440 nm. There were clear isosbestic points, indicative of a clean isomerization reaction about the azo group. Complex **3** behaved in a similar way.

The UV−visible spectrum of *trans*-**4** gave a peak at 342 nm corresponding to the expected $\pi-\pi^*$ transition, as shown in Figure 10. Upon irradiation with light at 365 nm, a decrease in

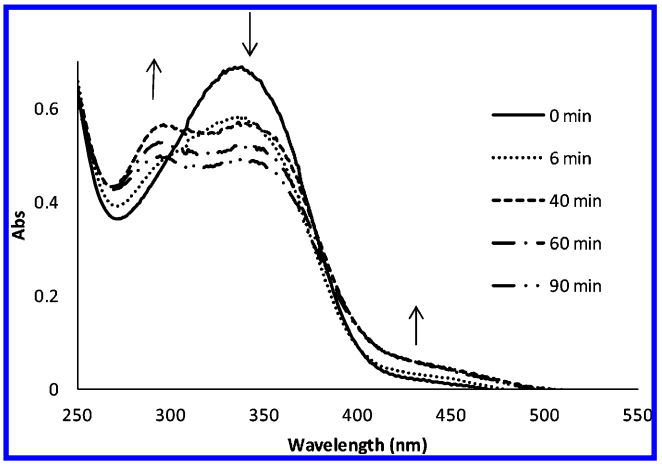

Figure 10. Absorption spectrum of [$PtIMe_3$(LL)] (**4**) in acetonitrile at 1.18 μM concentration for *trans*−*cis* photoisomerization upon illumination with UV light at 365 nm.

this band was noticed, and the corresponding growth of a peak at 435 nm is consistent with formation of the *cis* isomer. However, a peak also grew in at 283 nm, and no isosbestic point was observed in this region. It is likely that the isomerization is accompanied by slow photochemical decomposition in this case. Photolysis of platinum(IV) complexes leading to reductive elimination or free radical substitution is well-known.[19,20]

Figure 11 illustrates some of the frontier orbitals for the ligand LL, the dimethylplatinum(II) complex **1**, and the platinum(IV) complex **4**. The intraligand n−π^* and $\pi-\pi^*$ transitions are accessible in all cases, with the $\pi-\pi^*$ transition typically having the greatest intensity for the *trans* azobenzene derivatives.[8] However, for complex **1** the Pt(5d)−π^* metal-to-

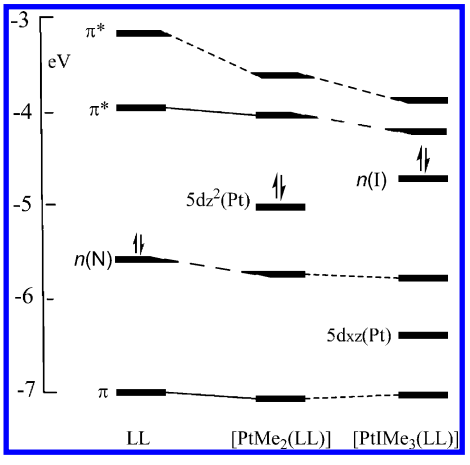

Figure 11. Calculated energies of the frontier orbitals in the ligand *trans*-LL and its complexes **1** and **4**.

dx.doi.org/10.1021/om3005405 | *Organometallics* 2012, 31, 6262−6269

ligand charge transfer band is at lower energy and has significant intensity (Figure 7). For the iodoplatinum(IV) complex **4** the I(5p)−π^* transition is expected to have the lowest energy, though the extinction coefficient is low (Figure 10), while the platinum 5d(π) orbitals are calculated to lie between the ligand n(N) and π levels (Figure 11). With irradiation at 365 nm, most absorption will lead to primary $\pi-\pi^*$ excitation (Figures 7, 9, and 10), though the other excited states can be accessible through internal conversion. The observation that all complexes **1**−**4** undergo *trans*−*cis* photoisomerization perhaps indicates that occupation of the π^* orbital is a sufficient condition to cause the *trans*−*cis* switching, but the back reaction is likely to be more affected by the other absorption bands close in energy to the n(N)−π^* transition for the *cis* isomers of the platinum complexes. The platinum(IV) complexes switch less efficiently than the platinum(II) complex **1**. The calculations suggest that the presence of platinum does not significantly affect the thermodynamics of the *trans*−*cis* isomerism. Thus, the preference for the *trans* over the *cis* isomer falls in the narrow range of 50−52 kJ mol^{-1} for the ligand LL and all of the platinum complexes **1**−**4**.

Monitoring the Photoisomerization Process by ^{1}H NMR. As a consequence of the difference in structure, the *trans* and *cis* isomers of azobenzene are expected to have considerable differences in the chemical shifts of the aromatic protons in the ^{1}H NMR spectra.[8] The photoisomerization of the azobenzene group in the complexes could therefore be monitored independently by ^{1}H NMR spectroscopy. Figure 12

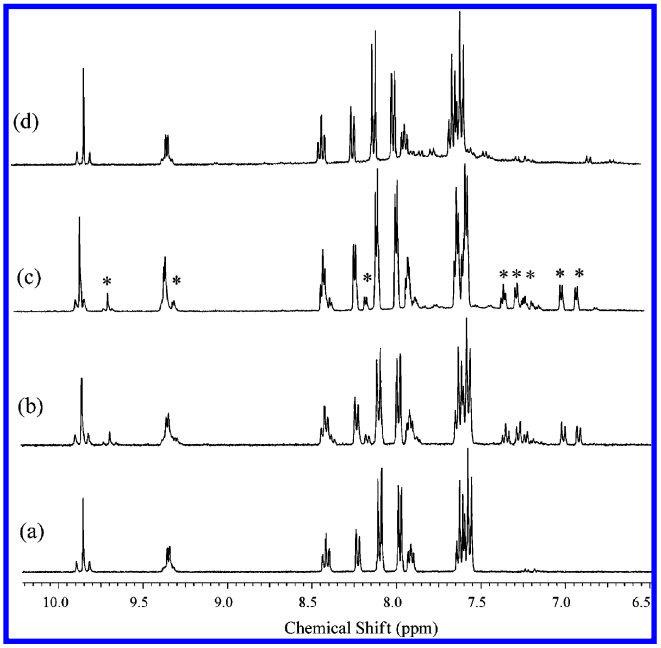

Figure 12. ^{1}H NMR spectra in the aromatic region of [$PtMe_2$(LL)] (**1**) in acetone-d_6, upon irradiation with UV light at 365 nm: (a) initial spectrum of *trans*-**1**; (b, c) after irradiation for 10 and 30 min, respectively; (d) after standing in the dark for 2 days. Peaks marked with asterisks are for the *cis* isomer.

shows the changes in the ^{1}H NMR spectrum of complex **1** upon irradiation with UV light to induce the *trans*−*cis* isomerization. An apparent equilibrium was obtained within 30 min of irradiation, giving a solution containing about 75% *trans*-**1** and 25% *cis*-**1**, and no further change was observed on extended irradiation at 365 nm (Figure 12b,c). The reverse *cis*−*trans* isomerization was confirmed by complete recovery and disappearance of the peaks for *trans*-**1** and *cis*-**1**, respectively, on keeping the NMR tube in the dark for 2 days (Figure 12a,d).

The analogous spectral changes on irradiation of the complex [$PtBr_2Me_2$(LL)] (**2**) are shown in Figure 13. Again the

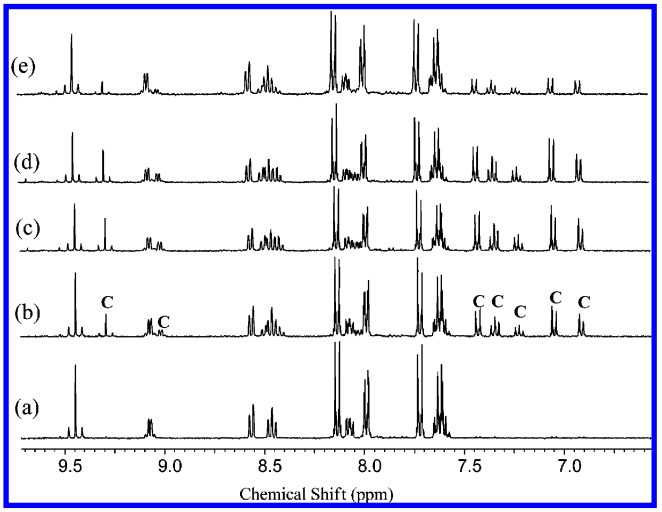

Figure 13. ^{1}H NMR spectral changes in the aromatic region of complex [$PtBr_2Me_2$(LL)] (**2**) in acetone-d_6, upon irradiation with UV light at 365 nm (c denotes resonances for the *cis* isomer); (a) spectrum of *trans*-**2** before irradiation; (b−d) after irradiation for 10, 20, and 40 min, respectively; (e) after standing in the dark for 2 days.

photolysis occurs to give an apparent equilibrium between *trans*-**2** and *cis*-**2**, this being complete in about 20 min of irradiation to give a solution containing about 60% *trans*-**2** and 40% *cis*-**2** (Figure 13b−d). There are changes in the chemical shifts of the aromatic protons similar to those observed for complex **1** (Figure 12). In this case, the reverse reaction was slower and was still incomplete after 2 days (Figure 13a,e). This behavior was typical of the platinum(IV) derivatives.

CONCLUSIONS

It has been shown that organoplatinum complexes containing the azo-based ligand 2-$C_5H_4NCH{=}N$-4-$C_6H_4N{=}NPh$ (LL) can undergo *trans*−*cis* isomerization of the azo group. The *trans*−*cis* isomerization is achieved by photolysis of the *trans* isomer using 365 nm incident light, while the reverse reaction occurs thermally, typically taking several days at room temperature. The conversion of *trans* to *cis* isomer is not quantitative because the *cis* isomer also absorbs, although with lower intensity, at 365 nm, thus leading to a photochemical steady state. The absorbance at 365 nm may have contributions from the azobenzene group but also from the platinum diimine group, and the π^* LUMO occupation can lead to *trans*−*cis* or *cis*−*trans* isomerization in either excited state. This complicating factor must be addressed in designing more efficient switching in organoplatinum complexes.

EXPERIMENTAL SECTION

All reactions were carried out under nitrogen using standard Schlenk techniques, unless otherwise specified. ^{1}H NMR spectra were recorded by using a Varian Mercury 400 spectrometer. UV−vis spectra were measured using a Varian Cary 300 Bio spectrophotometer. A sample of the ligand LL or complex was dissolved in acetonitrile and irradiated in a quartz cuvette at room temperature with UV light at 365 nm, followed immediately by recording the absorption spectrum. The

dx.doi.org/10.1021/om3005405 | *Organometallics* 2012, 31, 6262−6269

complex $[Pt_2Me_4(\mu\text{-}SMe_2)_2]$ and ligand 2-C_5H_4NCH=N-4-C_6H_4N=NPh (LL) were prepared according to the literature.[15,16] The ligand LL was isolated as an orange solid in 82% yield. ^{1}H NMR in $CDCl_3$: δ 8.76 (d, 1H, Py-H^6, $^3J_{HH}$ = 5 Hz), 8.66 (s, 1H, HC=N), 8.26 (d, 1H, $^3J_{HH}$ = 8 Hz), 8.01 (d, 2H, $^3J_{HH}$ = 8 Hz), 7.95 (d, 2H, $^3J_{HH}$ = 8 Hz), 7.87 (t, 2H, Py-H^{3,4}, J_{HH} = 8 Hz), 7.53−7.68 (m, 2H), 7.44 (d, 3H, $^3J_{HH}$ = 8 Hz). HRMS (ESI): calcd for $C_{18}H_{14}N_4$ $[M]^+$ 286.1218, found 286.1217.

X-ray Structure Determinations. Single crystals were grown from acetone/*n*-pentane at ambient temperature. A suitable crystal of each compound was coated in Paratone oil and mounted on a glass fiber loop. X-ray data for compounds **2** and **3** were collected at 150 K with ω and φ scans using a Bruker Smart Apex II diffractometer with graphite-monochromated Mo Kα radiation (λ = 0.710 73 Å) and Bruker SMART software.[21a] Unit cell parameters were calculated and refined from the full data set. Cell refinement and data reduction were performed using the Bruker APEX2 and SAINT programs, respectively.[21b] Reflections were scaled and corrected for absorption effects using SADABS.[21c] X-ray data for compound **4** were collected at 150 K with ω and φ scans on a Nonius Kappa-CCD diffractometer using graphite-monochromated Mo Kα radiation (λ = 0.710 73 Å) and COLLECT software.[21d] Unit cell parameters were calculated and refined from the full data set. Cell refinement and data reduction were performed using the DENZO-SMN software programs.[21e] Reflections were scaled and corrected for absorption effects using DENZO-SMN.[21e] All structures were solved by either Patterson or direct methods with SHELXS and refined by full-matrix least-squares techniques against F^2 using SHELXL.[21f] All non-hydrogen atoms were refined anisotropically. The hydrogen atoms were placed in calculated positions and refined using the riding model.

Only one of the structure refinements requires a comment. The unit cell of complex **2** contained a disordered pentane solvent molecule, for which no suitable model could be found. The electron density for this molecule was removed from the reflection data using SQUEEZE (PLATON), leaving a void of 206 Å^3. The electron density of 41e corresponds well to a pentane molecule (42e).

The crystals of complex **3** were grown from a solution of complex **1** with excess iodine in dichloromethane, by slow diffusion of pentane, and contained a molecule of iodine in the lattice.

DFT Calculations. DFT calculations were carried out by using the Amsterdam Density Functional program based on the BLYP functional, with first-order scalar relativistic corrections and double-ζ basis set.[22] All ground-state structures were confirmed to be energy minima by analysis of force constants for normal vibrations.[22]

[PtMe$_2$(LL)] (1). To a stirred solution of LL (0.5 g, 1.75 mmol) in toluene (20 mL) was added $[Pt_2Me_4(\mu\text{-}SMe_2)_2]$ (0.503 g, 0.875 mmol). After 10 min of stirring, a violet solid started to precipitate. The reaction mixture was stirred for 1 h, and the solid complex was collected by filtration, washed with ether (3 × 2 mL) and pentane (3 × 2 mL), and dried under high vacuum. Yield: 95% (0.848 g). ^{1}H NMR in acetone-d_6: δ 9.85 (s, 1H, $^3J_{PtH}$ = 30 Hz, CH=N), 9.35 (d, 1H, $^3J_{PtH}$ = 22 Hz, $^3J_{HH}$ = 6 Hz, Py-H^6), 8.42 (m, 1H, Py-H^4), 8.23 (d, 1H, $^3J_{HH}$ = 8 Hz, Py-H^3), 8.09 (d, 2H, $^3J_{HH}$ = 8 Hz, C_6H_4), 7.98 (d, 2H $^3J_{HH}$ = 8 Hz, *o*-Ph), 7.91 (m, 1H, Py-H^5), 7.53 (d, 2H, $^3J_{HH}$ = 8 Hz, C_6H_4), −7.67 (m, 3H, *m*,*p*-Ph), 1.31 (s, 3H, $^2J_{PtH}$ = 88 Hz, PtMe), 0.93 (s, 3H, $^2J_{PtH}$ = 88 Hz, PtMe). HRMS (ESI): calcd. For $C_{20}H_{20}N_4NaPt$ $[M]^+$ 534.1233, found 534.1234. ^{1}H NMR for *cis*-**1** in acetone-d_6: δ 9.66 (s, 1H, $^3J_{PtH}$ = 28 Hz, CH=N), 9.28 (d, 1H, $^3J_{PtH}$ = 19 Hz, $^3J_{HH}$ = 5 Hz, Py-H^6), 8.35 (m, 1H, Py-H^4), 8.14 (d, 1H, $^3J_{HH}$ = 7 Hz, Py-H^3), 7.84 (m, 1H, Py-H^5), 7.33 (m, 2H, *m*-Ph), 7.25 (d, 2H, $^3J_{HH}$ = 8 Hz, C_6H_4), 7.21 (m, 1H, *p*-Ph), 6.98 (d, 2H, $^3J_{HH}$ = 8 Hz, C_6H_4), 6.89 (d, 2H, $^3J_{HH}$ = 8 Hz, *o*-Ph), 1.22 (s, 3H, $^2J_{PtH}$ = 88 Hz, PtMe), 0.84 (s, 3H, $^2J_{PtH}$ = 88 Hz, PtMe).

[PtBr$_2$Me$_2$(LL)] (2). To a stirred solution of complex **1** (0.05 g, 0.095 mmol) in dry CH_2Cl_2 was added bromine (25 μL, 0.95 mmol). The solution changed from violet to red. The reaction mixture was stirred for 1 h., the volume of the solution was reduced to 1 mL, and pentane (10 mL) was added to precipitate a brown solid, which was separated by filtration, washed with ether (3 × 2 mL) and pentane (3 × 2 mL), and dried under vacuum. Yield: 85% (0.056 g). ^{1}H NMR in acetone-d_6: δ 9.44 (s, 1 H, $^2J_{PtH}$ = 26 Hz, CH=N), 9.07 (d, 1 H, $^3J_{PtH}$ = 18 Hz, $^3J_{HH}$ = 5 Hz, Py-H^6), 8.56 (d, 1H, $^3J_{HH}$ = 8 Hz, Py-H^3), 8.46 (m, 1H, $^3J_{HH}$ = 8 Hz, Py-H^4), 8.13 (d, 2H, $^3J_{HH}$ = 9 Hz, Ar-H), 8.07 (m, 1H, Py-H^5), 7.96−8.01 (m, 2H, Ar-H), 7.72 (d, 2H, $^3J_{HH}$ = 6 Hz, Ar-H), 7.58−7.66 (m, 3H, Ar-H), 2.06 (s, 3H, $^2J_{PtH}$ = 73 Hz, PtMe), 1.77 (s, 3H, $^2J_{PtH}$ = 72 Hz, PtMe). ^{1}H NMR for *cis*-**2** in acetone-d_6: δ 9.29 (s, 1H, $^2J_{PtH}$ = 27 Hz, CH=N), 9.03 (d, 1H, $^3J_{PtH}$ = 21 Hz, $^3J_{HH}$ = 5 Hz, Py-H^6), 8.49 (m, 1H, Py-H^5), 8.40 (m, 1H, Py-H^4), 8.03 (d, 1H, $^3J_{HH}$ = 7 Hz, Py-H^3), 7.44 (m, 2H, *m*-Ph), 7.36 (m, 1H, *p*-Ph), 7.24 (d, 2H, $^3J_{HH}$ = 9 Hz, C_6H_4), 7.06 (d, 2H, $^3J_{HH}$ = 9 Hz, C_6H_4), 6.92 (d, 2H, $^3J_{HH}$ = 9 Hz, *o*-Ph), 2.03 (s, 3H, $^2J_{PtH}$ = 73 Hz, PtMe), 1.64 (s, 3H, $^2J_{PtH}$ = 73 Hz, PtMe).

[PtI$_2$Me$_2$(LL)] (3). To a stirred solution of [PtMe$_2$(LL)] (**1**; 0.07 g, 0.137 mmol) in CH_2Cl_2 (20 mL) was added iodine (0.174 g, 1.37 mmol). An immediate color change of the solution from violet to red occurred with precipitation of a brown solid. The reaction mixture was stirred for 1 h, and the solid was collected and washed with pentane (3 × 2 mL) and was dried under vacuum. Yield: 89% (0.093 g). ^{1}H NMR in acetone-d_6: δ 8.89 (s, 1H, $^3J_{PtH}$ = 28 Hz, CH=N), 8.69 (d, 1H, $^3J_{PtH}$ = 19 Hz, $^3J_{HH}$ = 6 Hz, Py-H^6), 8.13 (d, 1H, $^3J_{HH}$ = 8 Hz, Py-H^3), 7.99 (m, 1H, Py-H^4), 7.70 (d, 2H, $^3J_{HH}$ = 9 Hz, Ar-H), 7.61 (m, 1H, Py-H^5), 7.55 (d, 2H, $^3J_{HH}$ = 8 Hz, Ar-H), 7.36 (d, 2H, $^3J_{HH}$ = 9 Hz, Ar-H), 7.18 (m, 3H, Ar-H), 1.96 (s, 3H, $^2J_{PtH}$ = 75 Hz, PtMe), 1.61 (s, 3H, $^2J_{PtH}$ = 75 Hz, PtMe).

[PtIMe$_3$(LL)] (4). To a solution of [PtMe$_2$(LL)] (0.075 g, 0.147 mmol) in acetone (20 mL) was added MeI (9 μL, 0.147 mmol). After 10 min the solution changed from purple to red with precipitation of a brown solid. The reaction mixture was stirred for 1 h, and the solid was collected and washed with pentane (3 × 2 mL) and dried under vacuum. Yield: 86% (0.083 g). ^{1}H NMR in acetone-d_6: δ 9.48 (s, 1 H, $^3J_{PtH}$ = 27 Hz, CH=N), 9.06 (d, 1 H, $^3J_{PtH}$ =18, $^3J_{HH}$ = 5 Hz, Py-H^6), 8.57 (d, 1H, $^3J_{HH}$ = 8 Hz, Py-H^3), 8.46 (m, 1H, Py-H^4), 8.14 (d, 2H, $^3J_{HH}$ = 9, Ar-H), 8.07 (m, 1 H, Py-H^5), 7.99 (d, 2H, $^3J_{HH}$ = 8 Hz, Ar-H), 7.73 (d, 2H, $^3J_{HH}$ = 9 Hz), 7.55−7.66 (m, 3H, Ar-H), 1.52 (s, 3H, $^2J_{PtH}$ = 73 Hz, PtMe), 1.18 (s, 3H, $^2J_{P-H}$ = 72 Hz, PtMe), 0.65 (s, 3H, $^2J_{PtH}$ = 72 Hz, PtMe). HRMS (ESI): calcd for $C_{21}H_{23}N_4NaPt$ $[M]^+$ 676.0513, found 676.0514.

[PtBrMe$_2$(CH$_2$Ph)(LL)] (5). To a solution of [PtMe$_2$(LL)] (**1**; 0.08 g, 0.156 mmol) in acetone (15 mL) was added benzyl bromide (0.019 μL, 0.156 mmol). Within 5 min, the color changed from violet to yellow with precipitation of the product as a brown solid. The solid was separated by filtration, washed with ether (3 × 2 mL) and pentane (3 × 2 mL), and dried under vacuum. Yield: 78% (0.083 g). ^{1}H NMR in acetone-d_6: δ 9.18 (d, 1H, $^3J_{PtH}$ = 27 Hz, CH=N), 8.74(d, 1H, $^3J_{PtH}$ =18 Hz, $^3J_{HH}$ = 6 Hz, Py-H^6), 8.26 (m, 2H, Py-H^5, Py-H^4), 8.03 (d, 2H, $^3J_{HH}$ = 9 Hz, Ar-H), 7.98 (d, 2H, *J* = 9 Hz, Ar-H), 7.7 (m, 1H, Py-H^3), 7.63−7.56 (m, 5H, Ar-H), 6.92 (d, 1H, $^3J_{HH}$ = 8 Hz, Ar-H), 6.85 (d, 2H, $^3J_{HH}$ = 7 Hz, Ar-H), 6.62 (d, 2H, $^3J_{HH}$ = 8 Hz, Ar-H), 2.80 (m, 1H, $^2J_{HH}$ = 14 Hz, $^2J_{PtH}$ = 96 Hz, PtCH$_2$), 2.65 (m, 1H, $^2J_{HH}$ = 14 Hz, $^2J_{Pt-H}$ = 78 Hz, PtCH$_2$), 1.52 (s, 3H, $^2J_{PtH}$ = 73 Hz, PtMe), 1.23 (s, 3 H, $^2J_{PtH}$ = 72 Hz, PtMe). HRMS (ESI): calcd for $C_{27}H_{27}BrN_4NaPt$ $[M]^+$ 703.0944, found 703.0963.

■ ASSOCIATED CONTENT

Ⓢ Supporting Information

CIF files giving X-ray data for the complexes. This material is available free of charge via the Internet at http://pubs.acs.org.

■ AUTHOR INFORMATION

Notes

The authors declare no competing financial interest.

■ ACKNOWLEDGMENTS

We thank the NSERC (Canada) for financial support.

REFERENCES

(1) (a) Natansohn, A.; Rochon, P. *Chem. Rev.* **2002**, *102*, 4139−4175. (b) Kawata, S.; Kawata, Y. *Chem. Rev.* **2000**, *100*, 1777−1788.

(2) (a) Matharu, A. S.; Jeeva, S.; Ramanujam, P. S. *Chem. Soc. Rev.* **2007**, *36*, 1868−1880. (b) Ikeda, T. *J. Mater. Chem.* **2003**, *13*, 2037−2057. (c) Kubo, S.; Gu, Z.-Z.; Takahashi, K.; Fujishima, A.; Segawa, H.; Sato, O. *J. Am. Chem. Soc.* **2004**, *126*, 8314−8319.

(3) (a) Dohno, C.; Uno, S. N.; Nakatani, K. *J. Am. Chem. Soc.* **2007**, *129*, 11898−11899. (b) Kano, N.; Komatsu, F.; Yamamura, M.; Kawashima, T. *J. Am. Chem. Soc.* **2006**, *128*, 7097−7109. (c) Archut, A.; Vögtle, F.; De Cola, L.; Azzellini, G. C.; Balzani, V.; Ramanujam, P. S.; Berg, R. H. *Chem. Eur. J.* **1998**, *4*, 699−706.

(4) Wang, S.; Songa, Y.; Jiang, L. C. *Photochem. Rev.* **2007**, *8*, 18−29.

(5) Orlandi, G. A.; Garavelli, M.; Tomasello, G.; Bearpark, J. M.; Robb, A. M.; Orlandi, G.; Gravellie, M. *Angew. Chem., Int. Ed.* **2010**, *49*, 2913−2916.

(6) Irie, M. *Chem. Rev.* **2000**, *100*, 1685−1716.

(7) Imaio, M.; Arai, T. *Tetrahedron Lett.* **2002**, *43*, 5265−5268.

(8) (a) Hampson, G. C.; Robertson, M. *J. Chem. Soc.* **1941**, 409−413. (b) Beharry, A. A.; Woolley, G. A. *Chem. Soc. Rev.* **2011**, *40*, 4422−4437. (c) Bandara, H. M. D.; Burdette, S. C. *Chem. Soc. Rev.* **2012**, *41*, 1809−1825. (d) Mourot, A.; Fehrentz, T.; Le Feuvre, Y.; Smith, C. M.; Herold, C.; Dalkara, D.; Nagy, F.; Trauner, D.; Kramer, R. H. *Nat. Methods* **2012**, *9*, 396. (e) Pandey, S.; Kolli, B.; Mishra, S. P.; Samui, A. B. *J. Polym. Sci. A* **2012**, *50*, 1205−1215. (f) Datta, S. N.; Pal, A. K.; Hansda, S.; Latif, I. A. *J. Phys. Chem. A* **2012**, *116*, 3304−3311.

(9) (a) Dogan, A.; Sarkar, B.; Klein, A.; Lissner, F.; Schleid, T.; Fiedler, J.; Zalis, S.; Jain, V. K.; Kaim, W. *Inorg. Chem.* **2004**, *43*, 5973−5980. (b) Kume, S.; Nishihara, H. *Dalton Trans.* **2008**, 3260−3271. (c) Han, M.; Hirade, T.; Hara, M. *New J. Chem.* **2010**, *34*, 2887−2891. (d) Michinobu, T.; Eto, R.; Kumazawa, H.; Fujii, N.; Shigehara, K. *J. Macromol. Sci. A* **2011**, *48*, 625−631. (e) Mallick, D.; Nandi, A.; Datta, S.; Sarker, K. K.; Mondal, T. P.; Sinha, C. *Polyhedron* **2012**, *31*, 506−514. (f) Samanta, S.; Ghosh, P.; Goswami, S. *Dalton Trans.* **2012**, *41*, 2213−2226. (g) Panja, A.; Matsuo, T.; Nagao, S.; Hirota, S. *Inorg. Chem.* **2011**, *50*, 11437−11445. (h) Inazuka, H.; Ogata, T.; Takeshita, K. *Kagaku Kogaku Ronbunshu* **2010**, *36*, 270−274. (i) Theilmann, O.; Saak, W.; Haase, D.; Beckhaus, R. *Organometallics* **2009**, *28*, 2799.

(10) (a) Ghedini, M.; Golemme, A.; Aiello, I.; Godbert, N.; Termine, R.; Crispini, A.; La Deda, M.; Lelj, F.; Amati, M.; Belviso, S. *J. Mater. Chem.* **2011**, *21*, 13434−13444. (b) Roy, S.; Hartenbach, I.; Sarkar, B. *Eur. J. Inorg. Chem.* **2009**, 2553−2558. (c) Ghedini, M.; Aiello, I.; Crispini, A.; Golemme, A.; La Deda, M.; Pucci, D. *Coord. Chem. Rev.* **2006**, *250*, 1373−1390. (d) Ghedini, M.; Pucci, D.; Crispini, A.; Barberio, G. *Organometallics* **1999**, *18*, 2116−2124. (e) Chattopadhyay, S.; Sinha, C.; Basu, P.; Chakravorty, A. *Organometallics* **1991**, *10*, 1135−1139. (f) Kaim, W. *Coord. Chem. Rev.* **2001**, *219*, 463−488.

(11) (a) Godbert, N.; Dattilo, D.; Termine, R.; Aiello, I.; Bellusci, A.; Crispini, A.; Golemme, A.; Ghedini, M. *Chem. Asian J.* **2009**, *4*, 1141−1146. (b) Ghedini, M.; Pucci, D.; Calogero, G.; Barigelletti, F. *Chem. Phys. Lett.* **1997**, *267*, 341−344. (c) Schneider, J. J.; Spickermann, D.; Bläser, D.; Boese, R.; Rademacher, P.; Labahn, T.; Magull, J.; Janiak, C.; Seidel, N.; Jacob, K. *Eur. J. Inorg. Chem.* **2001**, 1371−1382.

(12) (a) Segorra-Maset, M. D.; van Leeuwen, P. W. N. M.; Freixa, Z. *Eur. J. Inorg. Chem.* **2010**, 2075−2078. (b) Einaga, Y.; Mikami, R.; Akitsu, T.; Li, G. M. *Thin Solid Films* **2005**, *493*, 230−236. (c) Yutaka, T.; Mori, I.; Kurihara, M.; Mizutani, J.; Tamai, N.; Kawai, T.; Irie, M.; Nishihara, H. *Inorg. Chem.* **2002**, *41*, 7143−7150. (d) Sun, S.-S.; Anspach, J. A.; Lees, A. J. *Inorg. Chem.* **2002**, *41*, 1862−1869. (e) Sakamoto, R.; Kume, S.; Sugimoto, M.; Nishihara, H. *Chem. Eur. J.* **2009**, *15*, 1429−1439.

(13) (a) Bardaji, M.; Barrio, M.; Espinet, P. *Dalton Trans.* **2011**, *40*, 2570−2577. (b) Tang, H.-S.; Zhu, N.; Yam, V. W. W. *Organometallics* **2007**, *26*, 22−25. (c) Gherab, K. N.; Gatri, R.; Hank, Z.; Dick, B.; Kutta, R.-J.; Winter, R.; Luc, J.; Sahraoui, B.; Fillaut, J.-L. *J. Mater. Chem.* **2010**, *20*, 2858−2864.

(14) (a) Safa, M. A.; Abo-Amer, A.; Borecki, A.; Cooper, B. F. T.; Puddephatt, R. J. *Organometallics* **2012**, *31*, 2675−2681. (b) Au, R. H. W.; Jennings, M. C.; Puddephatt, R. J. *Dalton Trans.* **2009**, 3519−3525. (c) Achar, S.; Vittal, J. J.; Puddephatt, R. J. *Organometallics* **1996**, *15*, 43−50. (d) Achar, S.; Puddephatt, R. J. *Chem. Commun.* **1994**, 1895−1896. (e) Hill, G. S.; Yap, G. P. A.; Puddephatt, R. J. *Organometallics* **1999**, *18*, 1408−1418. (f) Monaghan, P. K.; Puddephatt, R. J. *Dalton Trans.* **1988**, 595−599. (g) Scott, J. D.; Puddephatt, R. J. *Organometallics* **1986**, *5*, 1538−1544. (h) Clark, H. C.; Puddephatt, R. J. *Inorg. Chem.* **1971**, *10*, 18.

(15) Chen, Z.-F.; Tang, Y.-Z.; Liang, H.; Fun, H.-K.; Yu, K.-B. *J. Coord. Chem.* **2006**, *59*, 207−214.

(16) (a) Hill, G. S.; Irwin, M. J.; Levy, C. J.; Rendina, L. M.; Puddephatt, R. J. *Inorg. Synth.* **1998**, *32*, 149−153. (b) Monaghan, P. K.; Puddephatt, R. J. *Organometallics* **1984**, *3*, 444−449.

(17) (a) Yahav, A.; Goldberg, I.; Vigalok, A. *Organometallics* **2005**, *24*, 5654. (b) Webb, J. R.; Munro-Leighton, C.; Pierpoint, A. W.; Gurkin, J. T.; Gunnoe, T. B.; Cundari, T. R.; Sabat, M.; Petersen, J. L.; Boyle, P. D. *Inorg. Chem.* **2011**, *50*, 4195−4211.

(18) Deplano, P.; Devillanova, F. A.; Ferraro, J. R.; Mercuri, M. L.; Lippolis, V.; Trogu, E. F. *Appl. Spectrosc.* **1994**, *48*, 1236.

(19) (a) Robinson, R.; Karikachery, A. R.; Sharp, P. R. *Dalton Trans.* **2012**, *41*, 2601−2611. (b) Castellano, F. N.; Pomestchenko, I. E.; Shikhova, E.; Hua, F.; Muro, M. L.; Rajapakse, N. *Coord. Chem. Rev.* **2006**, *250*, 1819−1828. (c) van Slageren, J.; Klein, A.; Zalis, S. *Coord. Chem. Rev.* **2002**, *230*, 193−211. (d) Yam, V.W.-W. *Chem. Commun.* **2001**, 789−790. (e) Connick, W. B.; Geiger, D.; Eisenberg, R. *Inorg. Chem.* **1999**, *38*, 3264−3265. (f) Chaudhury, N.; Puddephatt, R. J. *J. Organomet. Chem.* **1975**, *84*, 105−115.

(20) (a) van Slageren, J.; Stufkens, D. J.; Zalis, S.; Klein, A. *Dalton Trans.* **2002**, 218−225. (b) Hux, J. E.; Puddephatt, R. J. *J. Organomet. Chem.* **1992**, *437*, 251−263. (c) Pourreau, D. B.; Geoffroy, G. L. *Adv. Organomet. Chem.* **1985**, *24*, 249. (d) Dogan, A.; Kavakli, C.; Sieger, M.; Niemeyer, M.; Sarkar, B.; Kaim, W. *Z. Anorg. Allg. Chem.* **2008**, *634*, 2527−2531.

(21) (a) *APEX 2, Crystallography software package*; Bruker AXS, Madison, WI, 2005. (b) *SAINT, Data Reduction Software*; Bruker AXS, Madison, WI, 1999. (c) Sheldrick, G. M. *SADABS version 2.01*; Bruker AXS, Madison, WI, 2006. (d) *COLLECT*; Nonius BV, Delft, The Netherlands, 1998. (e) Otwinowski, Z.; Minor, W. *Methods Enzymol.* **1997**, *276*, 307−326. (f) Sheldrick, G. M. *Acta Crystallogr., Sect. A* **2008**, *64A*, 112−122.

(22) (a) Te Velde, G.; Bickelhaupt, F. M.; Baerends, E. J.; van Gisbergen, S.; Guerra, C. F.; Snijders, J. G.; Ziegler, T. *J. Comput. Chem.* **2001**, *22*, 931. (b) Becke, A. *Phys. Rev. A* **1988**, *38*, 3098.